RSC Advances

PAPER

View Article Online
View Journal | View Issue

Cite this: *RSC Adv.*, 2014, **4**, 40958

Discrete polynuclear manganese nanorods: syntheses, crystal structures and magnetic properties†

Jian-Jun Liu,[a] Yao Wang,[a] Shu-Ting Wu,[a] Mei-Jin Lin,*[ab] Chang-Cang Huang*[a] and Wen-Xin Dai[a]

Received 12th July 2014
Accepted 26th August 2014

DOI: 10.1039/c4ra07015a

www.rsc.org/advances

Shape-anisotropic nanomaterials with uniform lengths and widths have attracted much interest but few of them are involved in self-assembled manganese complexes. The combination of two redox-active acylthiosemicarbazide ligands with Mn^{3+} cations leads to two discrete polynuclear Mn nanorods, pentanuclear $[Mn_5(L3)_6][Mn_{0.7}(DMF)_{1.4}(H_2O)_{2.8}]$ (**1a**) and trinuclear $Mn_3(L4)_3\cdot 2DMF$ (**2**), whose L3 and L4 represent *N*-(5-(2-hydroxyphenyl)-1,3,4-oxadiazol-2-yl)benzamide and *N*-(5-(2-hydroxyphenyl)-1,3,4-oxadiazol-2-yl)-propionamide, respectively, which are *in situ* synthesized from their acylthiosemicarbazide derivatives in the presence of Mn^{3+} cations, while the latter are reduced into divalent ones in rod-like moieties. For each pentanuclear anion in **1a**, the charge is balanced by a solvated trivalent manganese cation, which can be replaced by two tetramethylammonium cations to yield pure valence compound **1b**. Moreover, the magnetic studies reveal all of them possess antiferromagnetic properties.

Introduction

One-dimensional magnetic nanomaterials (nanorods and nanowires) have attracted much interest in the past decades due to their potential applications in molecular switches,[1] data-storage devices,[2] site-specific drug release.[3] The shape anisotropy in one-dimensional nanostructures can result in a significantly increased coercivity, which can be tuned by adjusting the aspect ratio.[4] However, synthetic challenges remain in creating such one-dimensional magnetic nanomaterials with uniform lengths and widths, which limits their scope for applications.

Supramolecular self-assembly is an emerging method for the synthesis of nanostructures.[5] In the past decades, a great variety of polynuclear rod-like complexes of transition metals, including cobalt, nickel, copper and iron, have been prepared, and their shape-dependent properties evaluated.[6] Manganese, divalent or trivalent cation, contains an unpaired electron in their complexes, which makes it an ideal candidate for magnetic materials.[7] To our surprise, so far only few examples involved in manganese rod-like complexes,[8] which may attributed to their highly redox activities during crystallizations. To prevent forming the mixed complexes with mixed valences that are difficult crystallized, redox-active organic ligands are suggested to be used.

Acylthiosemicarbazide derivatives are an attractive class of multidentate ligands for the polynuclear complexes.[9] At the same time, they are also redox-active compounds.[10] According to the literature reported by Li and coworkers,[11] the acylthiosemicarbazide derivatives can undergo a ring closure process to form 2-amino-1,3,4-oxadiazole derivatives in the presence of metal oxidants. Thus, we selected such redox-active acylthiosemicarbazide as the parent core for our organic ligands. To increase their coordination dentations, the 2-hydroxyl phenyl and the second acyl groups have been incorporated into the acylthiosemicarbazide core, which is anticipated to afford the tetradentate oxadiazol ligands after the ring closure reactions. Analysis of the formed oxadiazol ligands reveals they can at least chelate with three manganese cations on the same line (Scheme 1). Herein, we indeed report two novel discrete polynuclear manganese nanorods (**1a** and **2**) by combining trivalent manganese cations with two acylthiosemicarbazide ligands, *N*-(2-(2-hydroxybenzoyl)hydrazinecarbonothioyl)benzamide (L1) and *N*-(2-(2-hydroxybenzoyl)hydrazine-carbonothioyl) propionamide (L2), respectively. In both nanorods, the manganese cations are reduced into the divalent ones, while the later ligands have transformed into their oxadiazol derivatives (L3 and L4) through a ring closure reaction in the presence of the oxidizer trivalent manganese cations. Interestingly, the complex **1a** bearing pentanuclear anionic nanorods is a mixed

[a]*College of Chemistry, Fuzhou University, 350116, China. E-mail: meijin_lin@fzu.edu.cn; cchuang@fzu.edu.cn; Tel: +86 591 2286 6143*

[b]*State Key Laboratory of Structural Chemistry, Fujian Institute of Research on the Structure of Matter, CAS, 350002, China*

† Electronic supplementary information (ESI) available: The detailed single crystal structures, characterization of L1 and L2, PXRD and bond length lists of complex of **1a**, **1b** and **2** as well as HRMS. CCDC 1009186–1009188. For ESI and crystallographic data in CIF or other electronic format see DOI: 10.1039/c4ra07015a

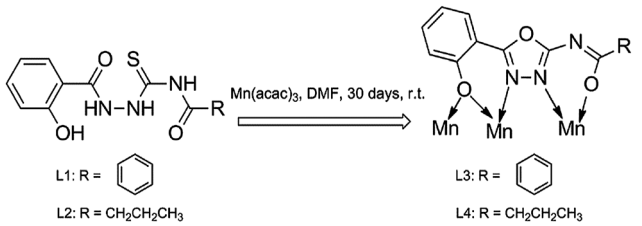

Scheme 1 The *in situ* syntheses of oxadiazole ligands from their acylthiosemicarbazide derivatives in the presence of Mn^{3+}. For clear explanation, a possible coordination pattern of such oxadiazole ligands is given.

valence compound possessing a black appearance, whose solvated trivalent manganese counter-cations can be replaced by tetramethylammonium cations to generate a yellow pure valence compound **1b**.

Experimental

Materials and measurements

N,*N*′-Dimetbylformamide (DMF, 99%), benzoyl chloride (99%), propionyl chloride (99%), potassium thiocyanate (analytical reagent grade), acetonitrile (analytical reagent grade), diethyl ether (analytical reagent grade), salicylhydrazide (99%), triethylamine (analytical reagent grade), tetramethylammonium chloride (98%) and manganese(III) acetylacetonate ($Mn(acac)_3$, 98%) were obtained from commercial suppliers. All chemicals and reagents were used as received unless otherwise stated. ^{1}H NMR spectra were recorded with a Bruker Avance 400 MHz NMR spectrometer. Chemical shifts are given in parts per million (ppm) and referred to TMS as internal standard. ^{1}H coupling constants J are given in Hertz (Hz). Powder X-ray diffraction (PXRD) intensities were recorded on a Rigaku MiniFlex-II X-Ray diffractometer with Cu Kα radiation (λ = 1.5406 Å) in the angular range of 2θ = 5–50° at 293 K. Mass spectra were recorded on a Thermo Fisher Scientific LCQ Fleet system. High-resolution mass spectra (HRMS) were acquired on the Thermo Scientific Exactive Plus Mass spectrometer equipped with an electrospray ionization (ESI) source. Magnetic susceptibility measurements for **1a** and **1b** were carried out on a Quantum Design MPMS XL7 SQUID magnetometer in the 2–300 K temperature range under magnetic field of 5000 Oe. Magnetic susceptibility data for **2** were collected over the temperature range of 2–300 K in magnetic field of 1000 Oe on a MPMS (SQUID)-XL magnetometer.

Synthesis

Synthesis of L1. Under the argon, benzoyl chloride (1.41 g, 10.0 mmol) was added to a solution of potassium thiocyanate (1.46 g, 15 mmol) in acetonitrile (30 mL), and the mixture was stirred for 3 hours at 70 °C, and then filtered affording a yellow filtrate. A portion of salicylhydrazide (1.52 g, 10.0 mmol) was added to the filtrate, and then further stirred for 3 hours at 70 °C to give a white precipitate, which was collected and rinsed with diethyl ether (2 × 30 mL). Yield: 85%. ^{1}H NMR (400 MHz, DMSO-d_6, ppm): δ = 13.72 (s, 1H), 12.00 (s, 1H), 11.96 (s, 1H), 11.88 (s, 1H), 8.02–7.00 (m, 9H). IR (KBr disk, ν cm^{-1}): 3410 (m), 3200 (m), 2950 (m), 1670 (s), 1523 (s), 1487 (m), 1280 (s), 1232 (m), 812 (s), 675 (m). HRMS (ESI$^-$) m/z calculated for $C_{15}H_{13}N_3O_3S$: 315.07; found: 314.06.

Synthesis of L2. L2 was prepared in a similar procedure as L1 by replacing benzoyl chloride with propionyl chloride. Yield: 70%. ^{1}H NMR (400 MHz, DMSO-d_6, ppm): δ = 13.41 (s, 1H), 11.85 (s, 2H), 11.66 (s, 1H), 7.97–7.00 (m, 4H), 2.47 (q, J = 8 Hz 2H), 1.06 (t, J = 8 Hz, 3H). IR (KBr disk, ν cm^{-1}): 3386 (w), 3262 (w), 3115 (s), 2982 (w), 1694 (s), 1622 (s), 1528 (m), 1474 (s), 1440 (s), 1203 (s), 1154 (s), 750 (s). HRMS (ESI$^-$) m/z calculated for $C_{11}H_{13}N_3O_3S$: 267.07; found: 266.06.

Synthesis of 1a. A portion of $Mn(acac)_3$ (0.071 mg, 0.2 mmol) and L1 (0.032 g, 0.1 mmol) were dissolved in 10 mL DMF, a drop of triethylamine was added and the solution was stirred for 3 h at room temperature. The resulting dark solution was filtered and the filtrate was left to stand at room temperature for about one month, during which time black crystals were produced in 25% yield based on Mn. Selected IR (KBr, cm^{-1}): 3150 (w), 2978 (w), 1650 (s), 1603 (s), 1484 (m), 1434 (m), 1265 (m), 1054 (m), 746 (s), 678 (s).

Synthesis of 1b. A portion of **1a** (0.230 g, 0.10 mmol) and tetramethylammonium chloride (0.109 g, 1 mmol) were dissolved in 5 mL DMF, and the clear solution was allowed to stand at ambient temperature for 10 days to give yellow single crystals of **1b**. Selected IR (KBr, cm^{-1}): 3342 (w), 3187 (m), 2985 (m), 1673 (s), 1625 (s), 1497 (m), 1454 (s), 1273 (m), 1158 (m), 745 (s), 665 (m).

Synthesis of 2. A portion of $Mn(acac)_3$ (0.071 mg, 0.2 mmol) and L2 (0.027 g, 0.1 mmol) were dissolved in 10 mL DMF, a drop of triethylamine was added and the solution was stirred for 3 h at room temperature. The resulting dark solution was filtered and the filtrate was left to stand at room temperature for about one month, during which time yellow crystals were produced in 18% yield based on Mn. Selected IR (KBr, cm^{-1}): 3248 (w), 3154 (w), 3052 (m), 2992 (m), 2948 (m), 2875 (w), 1666 (m), 1607 (s), 1558 (s), 1509 (s), 1484 (s), 1405 (s), 1332 (m), 1268 (s), 1096 (m), 973 (w), 860 (m), 752 (m), 614 (w).

X-ray diffraction analysis

Suitable single crystals of **1a**, **1b** and **2** were mounted on glass fibers for the X-ray measurement. Diffraction data were collected on a Rigaku-AFC7 equipped with a Rigaku Saturn CCD area-detector system. The measurement was made by using graphic monochromatic Mo Kα radiation (λ = 0.71073 Å) at 113 K under a cold nitrogen stream. The frame data were integrated and absorption correction using a Rigaku CrystalClear program package.[12] All calculations were performed with the SHELXTL-97 program package,[13] and structures were solved by direct methods and refined by full-matrix least-squares based on F^2. The non-hydrogen atoms were refined anisotropically. The hydrogen atoms were located by geometrical calculations except for those on the water molecules which were located from the difference Fourier syntheses. For the **1a** and **1b**, some included solvents were disorder and thus their contributions were

Table 1 Crystal data and structure refinement parameters for **1a**, **1b**, and **2**[a,b]

Complexes	**1a**	**1b**	**2**
Crystal size (mm)	0.38 × 0.25 × 0.20	0.35 × 0.26 × 0.24	0.23 × 0.18 × 0.15
Empirical formula	$C_{94.2}H_{69.4}Mn_{5.7}N_{19.4}O_{22.8}$	$C_{98}H_{78}Mn_5N_{20}O_{18}$	$C_{39}H_{47}Mn_3N_{11}O_{14}$
Formula weight	2151.05	2098.50	1058.70
Crystal system	Monoclinic	Monoclinic	Monoclinic
Space group	$P2_1/c$	$P2_1/c$	$P2_1/c$
a (Å)	12.205(2)	11.879(2)	11.609(2)
b (Å)	33.209(7)	31.352(6)	21.154(4)
c (Å)	14.952(3)	16.426(3)	18.246(4)
α (°)	90	90	90
β (°)	94.15(3)	94.25(3)	100.68(3)
γ (°)	90	90	90
V (Å^3)	6045(2)	6101(2)	4403.4(15)
Z	2	2	4
D_c (g cm^{-3})	1.182	1.142	1.597
μ(Mo Kα) (mm^{-1})	0.644	0.566	0.927
F(000)	2191	2150	2180
Collected reflections	48 925	42 602	36833
Independent reflections	13760	10 702	10073
Goodness-of-fit on F^2	1.098	1.107	1.219
R_1[a], wR_2[b] ($I > 2\sigma(I)$)	0.0924, 0.2551	0.0728, 0.1832	0.0639, 0.1147
R_1[a], wR_2[b] (all data)	0.1132, 0.2740	0.0885, 0.1932	0.0737, 0.1186

[a] $R_1 = \Sigma||F_o| - |F_c||/\Sigma|F_o|$. [b] $wR_2 = [\Sigma w(F_o^2 - F_c^2)^2/\Sigma w(F_o^2)]^{1/2}$.

subtracted from the data using SQUEEZE from the PLATON package of crystallographic software (Table 1).[14]

Results and discussions

Synthesis

As mentioned above, acylthiosemicarbazide derivatives have been reported to be cyclized into their corresponding oxadiazoles by metal or metal-free oxidants at elevated temperatures. Indeed, in our case, the organic ligands L1 and L2 are oxidized into oxadiazole building blocks L3 and L4 in the presence of Mn^{3+} to yield the final polynuclear nanorods whose manganese are reduced into divalent cations (for details, see the single-crystal structural description part in the following). The formation of oxadiazole building blocks as well as polynuclear nanorods is confirmed by the high-resolution mass spectral studies. For example, the HRMS of **1a** in *N*,*N*-dimethylformamide at 293 K shows a divalent anionic *m*/*z* peak at 975.04 and monovalent anionic *m*/*z* peak at 1950.08 (Fig. S5, ESI†), which correspond to theoretical distributions of polynuclear rod-like $[Mn_5(L3)_6]^{2-}$ and $[Mn_5(L3)_6]^{-}$ anions. It is also worthy pointing out that such *in situ* synthesis of oxadiazole ligands is supposed to play a key role in the formation of the final crystalline products since no target crystalline materials were obtained by the direct combination of L3 or L4 with Mn^{2+} or Mn^{3+}. Moreover, the addition of a catalytic amount of triethylamine to crystallization solutions is to facilitate deprotonation of acylthiosemicarbazide derivatives during cyclization reactions.

Single-crystal structural descriptions

Single crystals of **1a** suitable for X-ray diffraction analysis were obtained by slow evaporation of a DMF solution of $Mn(acac)_3$ and L1 at ambient temperature. The single crystal X-ray diffraction analysis revealed that it is crystallized in the monoclinic space group $P2_1/c$. In the crystalline **1a**, each smallest repetitive unit contains one pentanuclear Mn anion and one solvated Mn cation with around 70% occupancy. In the pentanuclear anionic parts, each Mn cation adopts a distorted octahedral coordination geometry to coordinate with three L3 ligands arranged along the same direction in a helical pattern through the formation of Mn–O or Mn–N bonds with a distance in the range 2.13–2.18 Å and 2.21–2.25 Å. Alternatively, each L3 ligand interconnects three Mn cations to form a $[Mn_2(L3)_3]$ dinuclear unit, which is self-coupled in a head–head model to yield the final pentanuclear clusters by sharing one Mn cation (Mn1) through Mn–O bonds (d_{Mn-O} = 2.16–2.18 Å) between Mn1 and O atoms from phenolate groups of oxadiazole building block L3. In pentanuclear clusters, the distances of Mn1 and Mn2, Mn2 and Mn3 are around 3.03 and 4.01 Å, respectively, while the angle of Mn1–Mn2–Mn3 is around 179.3°, which indicates the clusters is rod-like. Interestingly, the size of such rod-like polynuclear clusters is within the range of the nanometer, thus they are nanorods. Considering all the bond lengths of Mn–N and Mn–O bonds fall in the range of those for the divalent Mn cations, a conjecture can be drawn that all the Mn cations in the pentanuclear rod-like anions are divalent. As a result, the charges of the whole rod-like anions are divalent. Indeed, the anionic nature of such pentanuclear nanorods is supported by the coexistence of solvated Mn cations in crystals (Fig. 1). For the cationic moieties, each Mn cation (Mn4) is surrounded by four O atoms from four crystalline waters in the square plane and two carbonyl O atoms from two DMF molecules in the axial directions. Around 70% occupancy observed in X-ray diffraction for the solvated Mn cation indicates that their

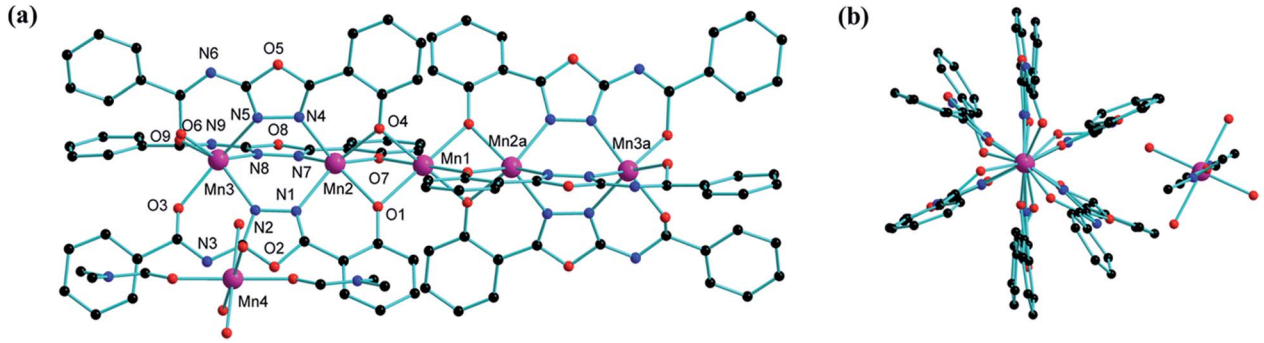

Fig. 1 Side view of the crystal structure of **1a** (a), as well as top view of the molecular structure of **1a** (b) (magenta Mn, blue N, red O, and black C). H atoms have been omitted for clarity.

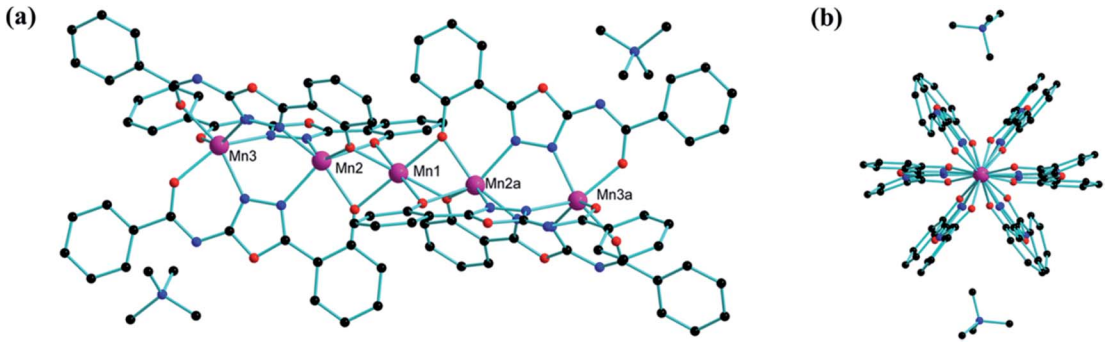

Fig. 2 Side view of the crystal structure of **1b** (a), as well as top view of the molecular structure of **1b** (b) (magenta Mn, blue N, red O, and black C). H atoms have been omitted for clarity.

Mn cations are trivalent, which is confirmed by the black appearance of crystal **1a** and the further experiment that each solvated Mn cation can be replaced by two monovalent tetramethylammonium cations (see below).

In general, the complex of Mn^{2+} is light color (yellow), however, **1a** is black. This may be attributed to the Mn4 is a trivalent cation in solvated Mn cations, which firstly can be deduced from their bond lengths and angles. In order to confirm our deduction, colourless tetramethylammonium chloride was selected as a proof-of-concept cation to replace the aforementioned solvated Mn4 cations owing to its close structural sizes. Co-crystallization of complex **1a** with tetramethylammonium chloride in DMF resulted in yellow prismatic crystals of **1b** after several days (Fig. S12, ESI†). Single-crystal X-ray diffraction analysis reveals that the anionic pentanuclear rod-like units in crystalline **1b** remain their structural features as in **1a**. However, the counter-cation of solvated Mn4 moieties are indeed replaced by two tetramethylammonium cations (Fig. 2), which corroborates our conjecture that the rod-like pentanuclear Mn nanorods are divalent anions, while the Mn cations in the solvated Mn4 units are +3 valence.

When the benzamide group in acylthiosemicarbazide ligand L3 is replaced by a flexible propionamide unit, similar combination of L4 with $Mn(acac)_3$ under the same conditions affords the yellow crystalline materials **2** suitable for X-ray diffraction analysis. Although the single crystal structural analysis revealed that complex **2** is also crystallized in the monoclinic space group $P2_1/c$, only one neutral trinuclear cluster composed of three Mn cations, three L4 ligands, three coordinated water and two free DMF molecules have been observed. From the yellow appearance of crystalline **2** (Fig. S12, ESI†), the Mn cations are supposed to be divalent. Similar as those in **1a** and **1b**, each Mn^{2+} cation in crystal **2** also adopting a distorted octahedral coordination geometry, is saturated by three O atoms and three N atoms, or six O atoms from three L4 ligands through Mn–O or Mn–N bonds (d_{Mn-O} = 2.14–2.19 Å and d_{Mn-N} = 2.22–2.27 Å) (Fig. 3). In other words, three L4 ligands arrange along the same direction to bridge three Mn^{2+} cations to form a pinwheel-like trinuclear coordination rod with a size close to 1 nm, where

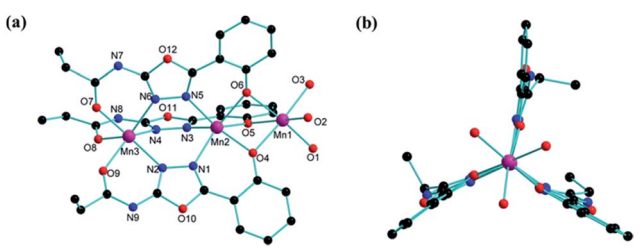

Fig. 3 Side view of the crystal structure of **2** (a), as well as top view of the molecular structure of **1a** (b) (magenta Mn, blue N, red O, and black C). H atoms have been omitted for clarity.

the distances between the neighboring two Mn^{2+} cations are around 3.02 Å and 4.06 Å, respectively, and the angle of three Mn^{2+} cations (Mn1–Mn2–Mn3) is *ca.* 177.6°. Different from **1a**, the left three coordination sites of the Mn1 cation that interconnects with three phenolate O atoms are terminated by three O atoms from three water molecules. As a result, these trinuclear clusters cannot further be self-coupled to generate higher nuclear rod-like complexes.

Magnetic properties

The magnetic measurements were carried out using a crystalline sample, whose phase purity was confirmed by powder X-ray diffraction (Fig. S6–S8, ESI†). The temperature-dependent magnetic susceptibility of crystalline **1a** and **1b** were investigated in the range of 2.0–300 K with a 5 kOe applied field (Fig. 4a and b). The magnetization *versus* field plot at 2.0 K is depicted in Fig. S13.† The $\chi_M T$ product of **1a** at 300 K is 22.96 cm^3 K mol^{-1}, which is slight lower than that for 0.7 Mn^{3+} ($S_{Mn^{3+}} = 2$) and five Mn^{2+} ($S_{Mn^{2+}} = 5/2$) cations magnetically noninteracting ($\chi_M T$ = 23.975 cm^3 K mol^{-1} with $g = 2.0$). With decreasing temperature, the $\chi_M T$ value decreases slowly and reaches 14.88 cm^3 K mol^{-1} at 10 K, after which it drops abruptly to a minimum value of 10.40 cm^3 K mol^{-1} at 2.0 K. The temperature dependence of molar susceptibility in the temperature range 50–300 K is well fitted by the Curie–Weiss law with $C = 24.58$ cm^3 K mol^{-1} and $\theta = -20.50$ K which indicates antiferromagnetic coupling between Mn cations.

For complex **1b**, the magnetic behavior upon cooling is slightly different from complex **1a**. Value of $\chi_M T$ at 300 K is 21.19 cm^3 K mol^{-1}, which is a bit smaller than expected for five non-interacting Mn(II) with $S = 5/2$ (21.875 cm^3 K mol^{-1}). The decline slope for $\chi_M T \sim T$ curve of complex **1b** in the range of 300 K to 10 K is similar to complex **1a**. A minimum $\chi_M T$ value (8.44 cm^3 K mol^{-1}) exists at 2 K. Curve of $\chi_M{}^{-1}$ *vs.* T follows Curie–Weiss law above 50 K, with Curie constant $C = 22.94$ cm^3 K mol^{-1} and Weiss constant $\theta = -26.08$ K, which indicates the antiferromagnetic property of complex **1b**.

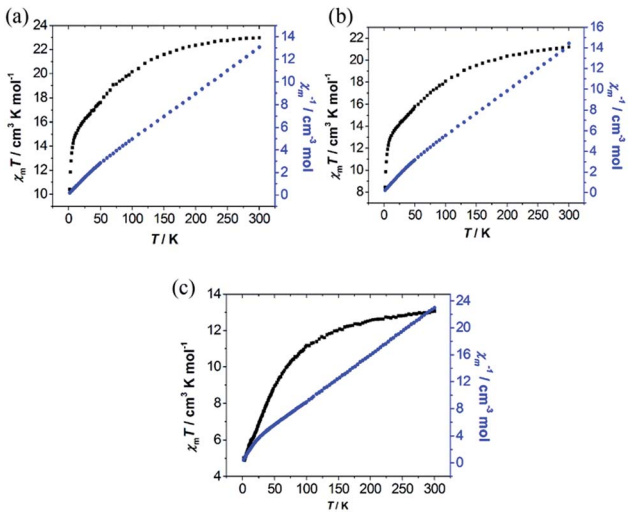

Fig. 4 Temperature dependence curves $\chi_M T$ *vs.* T (■) and $\chi_M{}^{-1}$ *vs.* T (●) for complex **1a** (a), **1b** (b) and **2** (c).

The variable-temperature magnetic susceptibility of crystalline **2** was investigated in the range of 2.0–300 K with a 1 kOe applied field. The magnetic properties of **2** in the form of $\chi_M T$ and $\chi_M{}^{-1}$ *versus* T plots are shown in Fig. 4c. At room temperature, $\chi_M T$ is equal to 13.06 cm^3 K mol^{-1}, which is close to theoretical value for three non-interacting Mn^{2+} with $S = 5/2$ (13.125 cm^3 K mol^{-1} with $g = 2.0$). The $\chi_M T$ value decreases gradually from room temperature to 11.16 cm^3 K mol^{-1} at 100 K and then sharply to 5.01 cm^3 K mol^{-1} at 2 K. The above data were fitted with Curie–Weiss law with $C = 14.28$ cm^3 K mol^{-1} and $\theta = -28.28$ K, which indicates antiferromagnetic coupling between Mn cations in **2**. By analyzing the magnetism of complexes **1a**, **1b**, and **2**, we can conclude that these compounds are antiferromagnetic coupling between Mn^{2+} cations. Similar magnetic phenomena have already been observed linear polynuclear complex with Mn^{2+} cations.[15]

Conclusions

In conclusion, we have demonstrated that the combination of two redox-active acylthiosemicarbazide ligands with trivalent manganese cations results in two discrete polynuclear manganese nanorods, whose organic building blocks are oxadiazol derivatives that are *in situ* synthesized from the added acylthiosemicarbazide ligands *via* a ring closure reaction in the presence of the oxidants trivalent manganese cations, while the latter are reduced into divalent ones in rod-like moieties. For the pentanuclear complex, the rod-like anions are balanced by the solvated trivalent manganese cations, which can be replaced by tetramethylammonium cations to generate a pure valence compound. In addition, the magnetic studies reveal all of three complexes possess antiferromagnetic properties, which may find applications in various directions.

Acknowledgements

We thank Prof. Jun-Dong Wang and Prof. Xin Fang for their useful discussions. This work has been supported by National Natural Science Foundation of China (21202020, 21273037), Doctoral Fund of Ministry of Education of China (20123514120002), Natural Science Foundation of Fujian Province (2014J01040 and 2014J01045), and Science & Technical Development Foundation of Fuzhou University (2012-XQ-10 and 2013-XQ-14).

Notes and references

1 (*a*) B. E. Feringa, *Molecular Switches*, Wiley-VCH, Weinheim, Germany, 2001; (*b*) A. Dei, D. Gatteschi, C. Sangregorio and L. Sorace, *Acc. Chem. Res.*, 2004, **37**, 827–835; (*c*) S. Yasuda, T. Nakamura, M. Matsumoto and H. Shigekawa, *J. Am. Chem. Soc.*, 2003, **125**, 16430–16433; (*d*) S. Yan, Z. Ding, N. Xie, H. Gong, Q. Sun, Y. Guo, X. Shan, S. Meng and X. Lu, *ACS Nano*, 2012, **6**, 4132–4136; (*e*) S. Tsoi, I. Griva, S. A. Trammell, A. S. Blum, J. M. Schnur and N. Lebedev, *ACS Nano*, 2008, **2**, 1289–1295.

2 (*a*) R. J. Tonucci, B. L. Justus, A. J. Campillo and C. E. Ford, *Science*, 1992, **258**, 783–785; (*b*) T. M. Whitney, P. C. Searson, J. S. Jiang and C. L. Chien, *Science*, 1993, **261**, 1316–1319; (*c*) A. Fert and L. Piraux, *J. Magn. Magn. Mater.*, 1999, **200**, 338–358; (*d*) A.-H. Lu, E. L. Salabas and F. Schuth, *Angew. Chem., Int. Ed.*, 2007, **46**, 1222–1244.

3 (*a*) H.-M. Fan, J.-B. Yi, Y. Yang, K.-W. Kho, H.-R. Tan, Z.-X. Shen, J. Ding, X.-W. Sun, M. C. Olivo and Y.-P. Feng, *ACS Nano*, 2009, **3**, 2798–2808; (*b*) S. D. Kong, W. Zhang, J. H. Lee, K. Brammer, R. Lal, M. Karin and S. Jin, *Nano Lett.*, 2010, **10**, 5088–5092; (*c*) G.-P. Li, Y.-X. Wang, Y.-F. Zhang and C.-F. Zhang, *Zhonghua Heyixue Zazhi*, 2007, **27**, 16–18.

4 (*a*) J. Park, B. Koo, Y. Hwang, C. Bae, K. An, J.-G. Park, H. M. Park and T. Hyeon, *Angew. Chem., Int. Ed.*, 2004, **43**, 2282–2285; (*b*) J. Park, B. Koo, K. Y. Yoon, Y. Hwang, M. Kang, J.-G. Park and T. Hyeon, *J. Am. Chem. Soc.*, 2005, **127**, 8433–8440; (*c*) K. A. Gregg, S. C. Perera, G. Lawes, S. Shinozaki and S. L. Brock, *Chem. Mater.*, 2006, **18**, 879–886; (*d*) C.-T. Lo and P.-Y. Kuo, *J. Phys. Chem. C*, 2010, **114**, 4808–4815.

5 (*a*) V. Georgakilas, F. Pellarini, M. Prato, D. M. Guldi, M. Melle-Franco and F. Zerbetto, *Proc. Natl. Acad. Sci. U. S. A.*, 2002, **99**, 5075–5080; (*b*) S. Kennedy, G. Karotsis, C. M. Beavers, S. J. Teat, E. K. Brechin and S. J. Dalgarno, *Angew. Chem., Int. Ed.*, 2010, **49**, 4205–4208; (*c*) X. Yan, S. Li, T. R. Cook, X. Ji, Y. Yao, J. B. Pollock, Y. Shi, G. Yu, J. Li, F. Huang and P. J. Stang, *J. Am. Chem. Soc.*, 2013, **135**, 14036–14039; (*d*) S. Huettner, M. Sommer, J. Hodgkiss, P. Kohn, T. Thurn-Albrecht, R. H. Friend, U. Steiner and M. Thelakkat, *ACS Nano*, 2011, **5**, 3506–3515.

6 (*a*) C.-H. Chien, J.-C. Chang, C.-Y. Yeh, L.-M. Fang, Y. Song and S.-M. Peng, *Dalton Trans.*, 2006, 3249–3256; (*b*) R. H. Ismayilov, W.-Z. Wang, G.-H. Lee, C.-Y. Yeh, S.-A. Hua, Y. Song, M.-M. Rohmer, M. Benard and S.-M. Peng, *Angew. Chem., Int. Ed.*, 2011, **50**, 2045–2048; (*c*) C. J. Matthews, S. T. Onions, G. Morata, L. J. Davis, S. L. Heath and D. J. Price, *Angew. Chem., Int. Ed.*, 2003, **42**, 3166–3169; (*d*) N. Sadhukhan, M. Sarkar, T. Ghatak, S. M. W. Rahaman, L. J. Barbour and J. K. Bera, *Inorg. Chem.*, 2013, **52**, 1432–1442.

7 (*a*) D. Gatteschi and R. Sessoli, *Angew. Chem., Int. Ed.*, 2003, **42**, 268–297; (*b*) C. J. Milios, A. Vinslava, W. Wernsdorfer, S. Moggach, S. Parsons, S. P. Perlepes, G. Christou and E. K. Brechin, *J. Am. Chem. Soc.*, 2007, **129**, 2754–2755; (*c*) C. J. Milios, A. Vinslava, P. A. Wood, S. Parsons, W. Wernsdorfer, G. Christou, S. P. Perlepes and E. K. Brechin, *J. Am. Chem. Soc.*, 2007, **129**, 8–9; (*d*) S. Zartilas, C. Papatriantafyllopoulou, T. C. Stamatatos, V. Nastopoulos, E. Cremades, E. Ruiz, G. Christou, C. Lampropoulos and A. J. Tasiopoulos, *Inorg. Chem.*, 2013, **52**, 12070–12079.

8 (*a*) R. A. Reynolds and D. Coucouvanis, *Inorg. Chem.*, 1998, **37**, 170–171; (*b*) S. K. Dey, T. S. M. Abedin, L. N. Dawe, S. S. Tandon, J. L. Collins, L. K. Thompson, A. V. Postnikov, M. S. Alam and P. Muller, *Inorg. Chem.*, 2007, **46**, 7767–7781.

9 (*a*) K.-K. Du and S.-X. Liu, *J. Mol. Struct.*, 2008, **874**, 138–144; (*b*) D. Dragancea, V. B. Arion, S. Shova, E. Rentschler and N. V. Gerbeleu, *Angew. Chem., Int. Ed.*, 2005, **44**, 7938–7942; (*c*) J.-J. Liu, J.-Z. Liao, Z.-Yi. Li, Y. Wang and C.-C. Huang, *Acta Crystallogr., Sect. C: Cryst. Struct. Commun.*, 2013, **69**, 613–615; (*d*) C.-C. Huang, J.-J. Liu, Y. Chen and M.-J. Lin, *Chem. Commun.*, 2013, **49**, 11512–11514.

10 (*a*) P. Gomez-Saiz, J. Garcia-Tojal, M. A. Maestro, F. J. Arnaiz and T. Rojo, *Inorg. Chem.*, 2002, **41**, 1345–1347; (*b*) E. Lopez-Torres and J. R. Dilworth, *Chem.–Eur. J.*, 2009, **15**, 3012–3023; (*c*) M. Sahin, A. Koca, N. Ozdemir, M. Dincer, O. Buyukgungor, T. Bal-Demirci and B. Ulkusevena, *Dalton Trans.*, 2010, **39**, 10228–10237; (*d*) P. S. Chaudhari, S. P. Pathare and K. G. Akamanchi, *J. Org. Chem.*, 2012, **77**, 3716–3723; (*e*) P. Gomez-Saiz, J. Garcia-Tojal, M. A. Maestro, J. Mahia, F. J. Arnaiz, L. Lezama and T. Rojo, *Eur. J. Inorg. Chem.*, 2003, 2639–2650; (*f*) A. Basu and G. Das, *Dalton Trans.*, 2011, **40**, 2837–2843.

11 X. Wang, Z. Li, B. Wei and J. Yang, *Synth. Commun.*, 2002, **32**, 1097–1103.

12 Rigaku, *Crystal Clear*, Rigaku Corporation, Tokyo, Japan, 2007.

13 G. M. Sheldrick, *Acta Crystallogr.*, 2008, **A64**, 112–122.

14 A. L. Spek, *PLATON, A Multipurpose Crystallographic Tool*, Utrecht University, Utrecht, The Netherlands, 2008.

15 (*a*) M. Kloskowski, D. Purschea, R.-D. Hoffmanna, R. Pöttgena, M. Lägea, A. Hammerschmidt, T. Glaserb and B. Krebs, *Z. Anorg. Allg. Chem.*, 2007, **633**, 106–112; (*b*) L. A. Barrios, G. Aromí, J. Ribas, J. S. Uber, O. Roubeau, K. Sakai, S. Masaoka, P. Gamez and J. Reedijk, *Eur. J. Inorg. Chem.*, 2008, 3871–3876.